THE JOURNAL OF PHYSICAL CHEMISTRY A

Article

pubs.acs.org/JPCA

Singlet Oxygen Generation on Porous Superhydrophobic Surfaces: Effect of Gas Flow and Sensitizer Wetting on Trapping Efficiency

Yuanyuan Zhao,[†] Yang Liu,[†] Qianfeng Xu,[†] Mark Barahman,[†] Dorota Bartusik,[‡] Alexander Greer,*[,‡] and Alan M. Lyons*[,†]

[†]Department of Chemistry, College of Staten Island, City University of New York, Staten Island, New York 10314, United States

[‡]Department of Chemistry, Brooklyn College, City University of New York, Brooklyn, New York 11210, United States

Supporting Information

ABSTRACT: We describe physical-organic studies of singlet oxygen generation and transport into an aqueous solution supported on superhydrophobic surfaces on which silicon–phthalocyanine (Pc) particles are immobilized. Singlet oxygen ($^1O_2$) was trapped by a water-soluble anthracene compound and monitored *in situ* using a UV–vis spectrometer. When oxygen flows through the porous superhydrophobic surface, singlet oxygen generated in the plastron (i.e., the gas layer beneath the liquid) is transported into the solution within gas bubbles, thereby increasing the liquid–gas surface area over which singlet oxygen can be trapped. Higher photooxidation rates were achieved in flowing oxygen, as compared to when the gas in the plastron was static. Superhydrophobic surfaces were also synthesized so that the Pc particles were located in contact with, or isolated from, the aqueous solution to evaluate the relative effectiveness of singlet oxygen generated in solution and the gas phase, respectively; singlet oxygen generated on particles wetted by the solution was trapped more efficiently than singlet oxygen generated in the plastron, even in the presence of flowing oxygen gas. A mechanism is proposed that explains how Pc particle wetting, plastron gas composition and flow rate as well as gas saturation of the aqueous solution affect singlet oxygen trapping efficiency. These stable superhydrophobic surfaces, which can physically isolate the photosensitizer particles from the solution may be of practical importance for delivering singlet oxygen for water purification and medical devices.

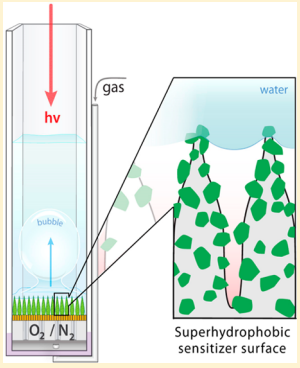

INTRODUCTION

Singlet oxygen ($^1O_2$) can be generated by photosensitized processes and can be used for many important applications.[1,2] A high pressure $^1O_2$ generator has been reported.[3] Other examples of $^1O_2$ generation include microfluidic or simple flow reactors in which $^1O_2$ photooxidation reactions are conducted by using dissolved or polymer-bound sensitizers.[3−9] Photodynamic therapy (PDT) applications have been demonstrated in vitro using sensitizer nanoparticles.[10] Reversible control of $^1O_2$ generation has been achieved with diarylethene photochromic switches.[11] The field continues to flourish with new kinds of sensitizer polymers and particles being reported.[12−14]

One challenge to using devices that generate $^1O_2$ is the potential for contamination. Either the sensitizer molecule is dispersed directly in the solution and so difficult to recover, or a solid sensitizer could dissolve, contaminating the solution. Similarly, the solution, photobleached sensitizer or other products of the photooxidation, could contaminate the sensitizer molecules or particle surfaces. Previously,[15] we described a SMA-type photoreactor device that bubbled oxygen gas enriched in $^1O_2$, where the sensitizer was isolated behind an ultrahigh molecular weight polyethylene membrane. More recently, we have shown[16] that photosensitizer particles can be embedded into a superhydrophobic surface and that singlet oxygen generated at the surface can be trapped in discrete droplets supported in the Cassie state[17] on the surface.

In this paper, we advance our work on triphasic superhydrophobic sensitizers[16] by incorporating the superhydrophobic surface into a new $^1O_2$ cuvette photoreactor device, as shown schematically in Figure 1. This design enables control over both the gas composition and gas flow rate through in the plastron (i.e., the gas layer below the liquid). The effect of oxygen concentration at the particle surface was studied systematically and in real time by measuring the concentration of $^1O_2$ trapped by 9,10-anthracene dipropionate dianion **1** *in situ* using UV–vis spectroscopy (Scheme 1). Our hypothesis is that flowing O_2 gas through the plastron will release $^1O_2$ bubbles into the supported liquid and increase the photooxidation rate compared to a static gas environment.

An understanding of the mechanism of $^1O_2$ formation in superhydrophobic sensitizers is key to $^1O_2$ utilization for various potential applications. To help achieve this mechanistic insight, three types of surfaces were prepared, as shown schematically in Figure 2, where the wetting of the particles by the solution was varied. Surface were prepared where sensitizer particles were dispersed across the entire surface (surface A),

Special Issue: Current Topics in Photochemistry

Received: March 30, 2014
Revised: June 2, 2014
Published: June 2, 2014

   dx.doi.org/10.1021/jp503149x | *J. Phys. Chem. A* 2014, 118, 10364−10371

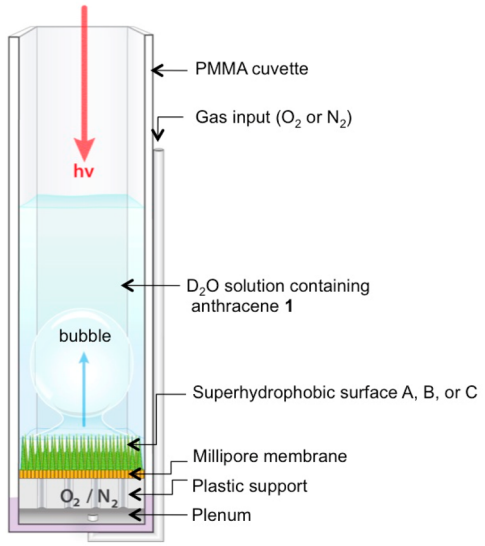

Figure 1. Geometry of the $^1O_2$ photoreactor device. A poly(methyl methacrylate) (PMMA) cuvette was modified to incorporate a superhydrophobic surface embedded with Pc particles printed onto a porous membrane. The printed membrane is held on a plastic support plate that defines the top of the plenum. Holes were drilled through the plate enabling gas to flow from the plenum to the plastron. A gas input needle inserted into the bottom of the plenum is used to introduce a controlled flow of gas.

Scheme 1

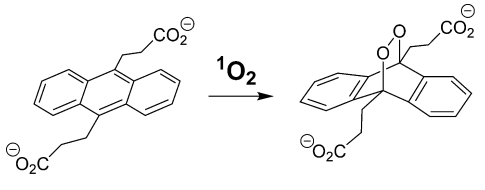

1 2

isolated at the tips of the posts in contact with the liquid layer (surface B), or physically separated from the liquid, exposed only in the plastron (surface C). Surfaces A–C exhibit stable superhydrophobic properties with a fully intact plastron throughout the experiment. On the basis of results from these surfaces, a photooxidation mechanism is proposed.

Another aim of this work is to demonstrate a system that researchers in the field of photooxidation chemistry can use to study sensitizer solids in controlled atmospheres that are not required to be fully wetted by the solution.[18] Essentially any particulate photosensitizer is compatible with the easy-to-use dispensable photoreactor described herein. By combining physical-organic chemistry principles with surface engineering techniques, we can control gas/liquid and gas/solid photooxidation reactions, which could benefit researchers across numerous fields. To our knowledge, no $^1O_2$-generating superhydrophobic surfaces with control of wetting and plastron gas composition have been previously reported.

EXPERIMENTAL SECTION

Reagents, Materials, and Instrumentation. Silicon phthalocyanine dichloride ($SiPcCl_2$), (3-aminopropyl)-triethoxysilane (ATPS), [3-(glycidyloxy)propyl]-trimethoxysilane (GPTMS), 9,10-anthracene dipropionic acid, potassium hydroxide, and D_2O were purchased from Sigma-Aldrich (Allentown, PA). The above chemicals were used as received without further purification. A 0.10 mM solution of 9,10-anthracene dipropionic acid was prepared in D_2O and the pH was adjusted to 10 with KOH to form a solution of 9,10-anthracene dipropionate dianion **1**. SiO_2 nanoparticles were received from Evonik (Aerosil R812S); a room-temperature vulcanizing (RTV) polydimethylsiloxane (PDMS) one-part adhesive manufactured by Dow Corning (3140) was purchased from Ellsworth Adhesives. The silicon phthalocyanine (Pc) glass particles (40–150 μm) were prepared as described previously.[15] Optical energy was delivered from a CW diode laser (669 nm output, 383 mW, Intense Ltd.). An optical fiber from the laser diode was brought into the cuvette with an incident angle of 90° to the surface. The peak in the absorption spectrum of the Pc particles occurred at 670 nm, nearly coincident with the laser line at 669 nm, to generate $^1O_2$ by energy transfer from triplet Pc excited sites to $^3O_2$.[19,20] SEM images were obtained using AMRAY 1910 Emission Scanning Electron Microscope.

Fabrication of Superhydrophobic Surfaces with Pc Particles in Controlled Locations. The process for printing PDMS posts was reported previously.[21,22] Briefly, the PDMS posts were printed as a 17 × 17 square array with a pitch of 0.5 mm (8 mm × 8 mm array) on a 10 mm × 10 mm membrane surface. Surfaces A–C were also reported previously.[16] For surface A, a layer of Pc particles was spread onto the posts immediately after printing. The viscous and thixotropic properties of the PDMS maintained their shape before cure; the Pc particles became partially embedded into the uncured surface ensuring good adhesion between the particles and the PDMS posts. The surface was cured at 65 °C for 2 h. Excess particles were removed by exposing the surface to high flows of compressed air.

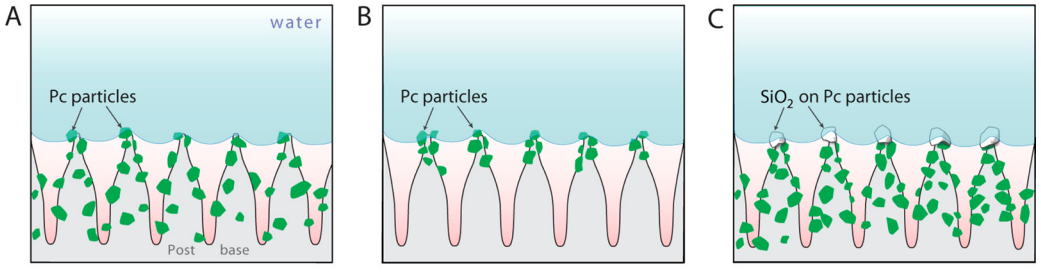

Figure 2. Schematic images of PDMS posts coated with Pc particles at controlled locations. (A) Surface A has Pc particles coating the PDMS posts. (B) Surface B has Pc particles primarily embedded at the PDMS tips. (C) Surface C has Pc coating the PDMS post base, where tips are capped with a layer of PDMS and SiO_2 nanoparticles.

dx.doi.org/10.1021/jp503149x | J. Phys. Chem. A 2014, 118, 10364–10371

Figure 3 shows a schematic of the fabrication of surface B. Here, immediately after printing the PDMS posts, the tips of

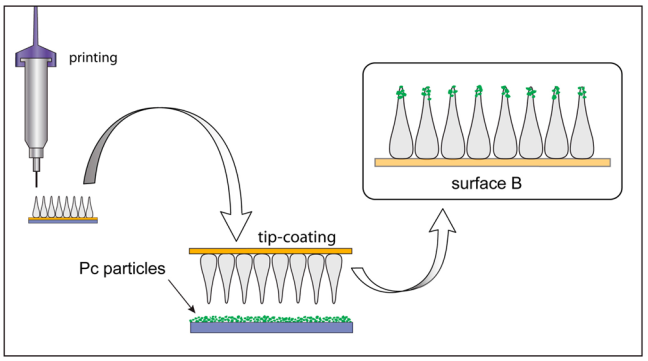

Figure 3. Schematic of the fabrication of surface B.

the posts were dipped into a thin layer of Pc particles. The tip-coated posts were cured at 65 °C in an oven with tips facing down.

Figure 4 shows a schematic of the fabrication of surface C. The PDMS post surface was printed and coated with Pc

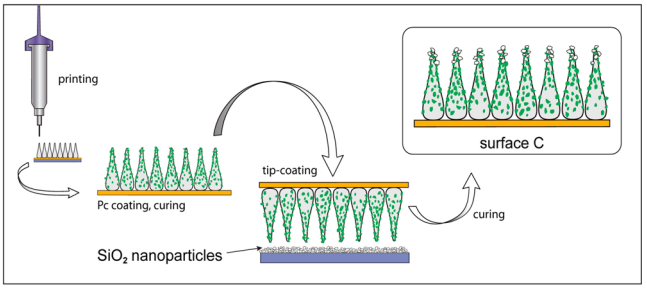

Figure 4. Schematic of the fabrication of surface C.

particles (as for surface A). After curing and removal of excess Pc particles, the tips were dipped into a thin layer of uncured PDMS approximately 200 μm thick. The surface was then dipped into a thin layer of SiO_2 nanoparticles such that the silica adhered to the uncured silicone. Finally, the post array was cured at 65 °C in an oven with tips facing down.

Figure 5 shows the SEM images of surfaces A–C showing the structure of the printed posts with Pc particles embedded on the surface. These surfaces have a course-scale primary roughness, which is formed by printing an array of PDMS posts (1 mm tall, 0.50 mm pitch). The Pc particles that are adhered to the uncured PDMS surface produce a secondary roughness, whereas a tertiary roughness is formed from the thin layer of SiO_2 nanoparticles (surface C).

$^1O_2$ Photoreactor Device. The bottom of a PMMA disposable cuvette was removed to enable connection to the superhydrophobic surfaces A-C. The PDMS posts were printed onto a Millipore membrane (10 mm × 10 mm) with a pore size of 0.5 μm, coated with particles and cured. The printed membrane was then placed on a 1 cm^2 Delrin plastic (3 mm thick) support plate that defined the top of the plenum. Five holes (1 mm diameter each) drilled through the plate enabled gas to flow from the plenum to the plastron. The support plate was inserted halfway into a 1 cm^2 custom-molded silicone rubber chamber (3 mm thick), leaving a 1.5 mm deep plenum for gas purging. A 25G 11/2 in. needle was bent and inserted into the bottom of the plenum with the silicone forming a gastight seal. The other end of the needle was connected to a regulated gas supply, where a flow rate of 20 cm^3/min was controlled with a rotameter.

In-Situ Measurements of Singlet Oxygen Produced by the Superhydrophobic Sensitizers. The cuvette was placed in an Ocean Optics cuvette holder fitted with optical fibers connected to a light source (Mikropack HL2000) and spectrometer (Ocean Optics USB4000) such that the solution absorption of **1** was measured *in situ* during irradiation from the top opening of the cuvette. In a few cases, absorption spectra were collected using a Perkin Elmer (Lambda 650) spectrophotometer. For the solution presaturation studies, stock solutions of **1** in D_2O (~20 mL) were purged in N_2 or O_2 for 2 h at 100 cm^3/min prior to transferring 2 mL portions to the photoreactor. For each plot, three different surfaces were fabricated and the photocatalysis reaction was measured to obtain the data reported in the graphs and tables. The average value and the standard deviation based on these three measurements are reported. By using a new surface for each measurement, we demonstrate the reproducibility of both the fabrication technique and the reaction results.

RESULTS AND DISCUSSION

Effect of Plastron Gas Composition and Flow. A series of experiments was conducted using surface A to evaluate the effect of gas flow, gas composition in the plastron, and dissolved oxygen concentration in the fluid on $^1O_2$ formation. Aqueous solutions form a stable Cassie state on these surfaces owing to the hierarchical roughness. A course scale primary roughness is formed by the high aspect ratio printed PDMS posts. These posts alone would form a superhydrophobic surface; however, partial wetting of the PDMS posts can occur.[21] Embedding Pc particles into the PDMS surface, however, increases the stability

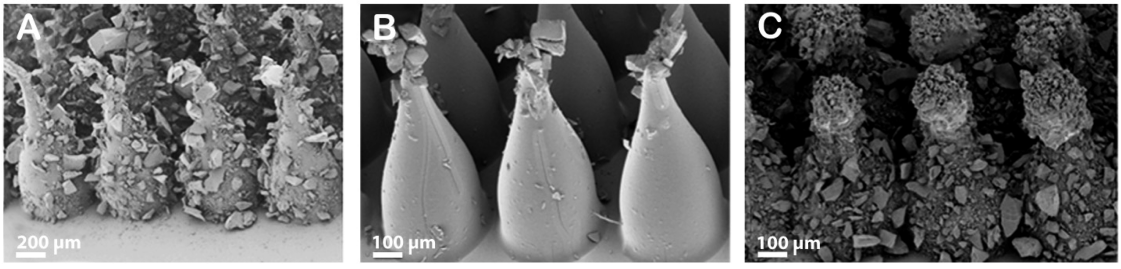

Figure 5. SEM images of PDMS posts coated with Pc particles at controlled locations: (A) surface A with particles coating the entire PDMS surface; (B) surface B with particles adhered only to the top portion of the PDMS posts; and (C) surface C where the surface prepared as in surface A was capped with a layer of silica nanoparticle adhered to a layer of PDMS.

dx.doi.org/10.1021/jp503149x | J. Phys. Chem. A 2014, 118, 10364–10371

of the Cassie state owing to the hydrophobic surface of the particles as well as the course particle morphology, which adds an additional level of roughness with re-entrant features to the surface. Such hierarchical roughness has been shown to increase the stability of superhydrophobic properties.[22,23] There was no encroachment of water into the post interstices (i.e., no Wenzel state).[24−26]

Data were collected by singlet oxygen trapping with 9,10-anthracene dipropionate dianion **1**, a specific $^1O_2$ reaction developed by Rodgers et al.,[27,28] as a facile and convincing $^1O_2$ reporter compound. By analogy, others[29−32] have detected $^1O_2$ by trapping with anthracene compounds, which lead to endoperoxides that can further decompose to radicals,[33] and an $^1O_2$ mechanism is indicated with Pc sensitizers (Type II process)[34] with a minimal contribution from Type I (radical) photooxidation reactions.[35,36] D_2O was used in favor of H_2O due to the 20-fold longer lifetime of $^1O_2$ (65 μs compared to 3.5 μs)[37] for rapid and reliable data collection, so that shorter reaction times were required.

Figure 6 shows the results of experiments with static air; i.e., no gas flowed through the plastron. D_2O solutions were

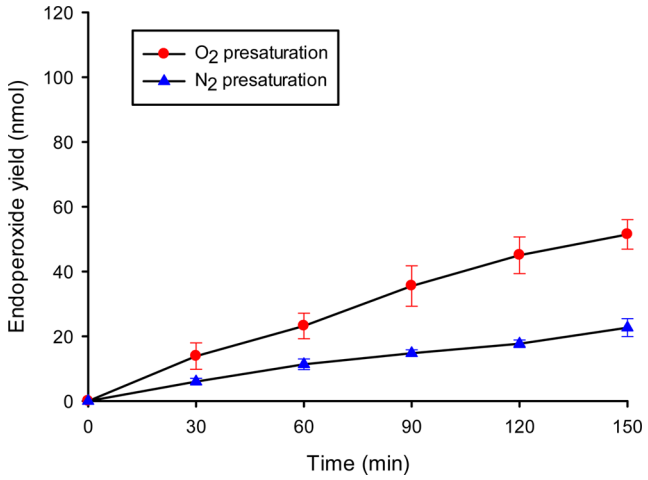

Figure 6. Endoperoxide **2** yield in static experiments where D_2O solutions were presaturated with O_2 or N_2. There was no gas sparging through the plenum of the device. Error bars represent the standard deviation obtained from 3 measurements.

presaturated with either $^3O_2$ or N_2 before being filled into the cuvette. With static air in the plastron, solutions presaturated with $^3O_2$ produced more than a 2-fold higher yield of endoperoxide **2** (51.5 nmol) compared to solutions presaturated with N_2 (22.7 nmol) after laser irradiation for 2.5 h. For the N_2 presaturated solutions, $^3O_2$ was available both from the plastron and from the top of the cuvette, which was open to air. Nonetheless, the rates can be seen to slow slightly after the first hour, indicating that oxygen was depleted from the system during the reaction.

Introducing a gas flow through the plastron significantly affects the yields of endoperoxide observed. Figure 7 shows optical images of the photoreactor equipped with surface A, in which a bubble forms at the plastron−liquid interface. As shown in a video (Supporting Information), bubbles grow from the plastron and then release and rise through the 2 mL D_2O solution. After bubble release, the plastron re-forms (Figure 7A,C) and the bubble growth and release cycle repeats continuously. The solution remains in the Cassie state throughout the experiment. Formation of bubbles increases the surface area and time over which the gas can dissolve into solution.

Figure 8 shows the results of experiments where gas was purged through the plastron; two effects were observed. First,

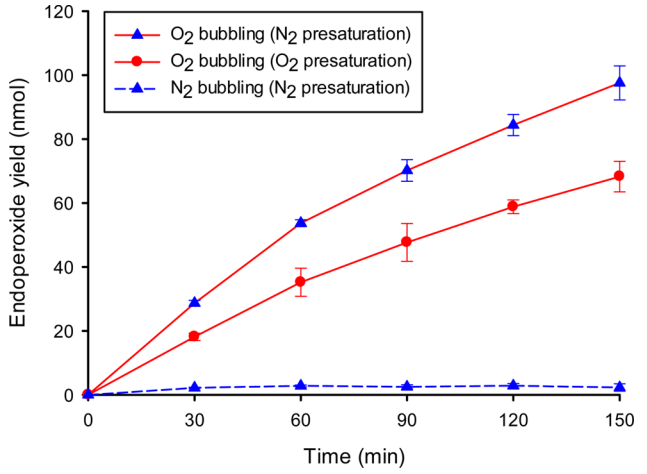

Figure 8. Endoperoxide **2** yield in bubbling experiments where O_2 or N_2 gas was sparged through the plenum into the D_2O solution. Error bars represent the standard deviation were obtained from three measurements.

the rate of endoperoxide formation was enhanced by the flow of $^3O_2$. The yield of endoperoxide **2** increased by >30% (from 51.5 to 68.3 nmol after 2.5 h) in flowing $^3O_2$ compared to when static air was maintained in the plastron. Second, the oxygen concentration in solution has an effect on $^1O_2$ trapping. Presaturating the D_2O solution with N_2 gas results in higher initial rates of $^1O_2$ trapping with an endoperoxide yield of 97.6 nmol, compared with a yield of 68.3 nmol in a solution presaturated with $^3O_2$. Although $^3O_2$ is necessary for $^1O_2$ formation, solutions presaturated with $^3O_2$ exhibit lower yields of endoperoxide **2**. When N_2 was bubbled through a solution

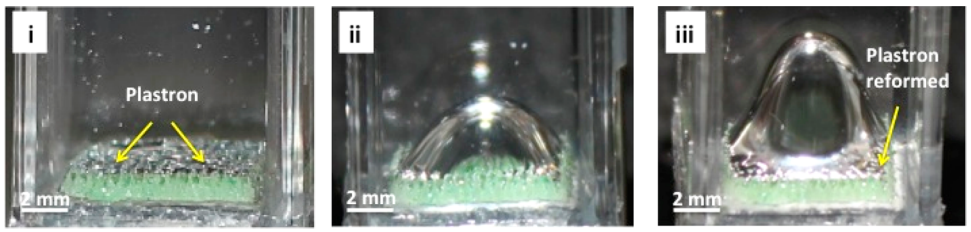

Figure 7. Optical images of surface A, showing (i) plastron with a planar and reflective air−water interface, (ii) gas bubble forming over the surface, and (iii) gas bubble releasing from the surface.

dx.doi.org/10.1021/jp503149x | J. Phys. Chem. A 2014, 118, 10364−10371

Table 1. Singlet Oxygen Trapping Experiments

gas flow	solution presaturated	percent decrease in anthracene 1 after 2.5 h (%)[a,c]	endoperoxide 2 formed (nmol)[c]	initial rate (nmol/min)[b,c]	final rate (nmol/min)[b,c]
O_2 purging	N_2	48.8 ± 2.7	97.6 ± 5.3	0.96 ± 0.03	0.22 ± 0.05
	O_2	34.2 ± 2.4	68.3 ± 4.8	0.60 ± 0.04	0.21 ± 0.07
static	N_2	11.4 ± 1.4	22.7 ± 2.8	0.20 ± 0.03	0.17 ± 0.05
	O_2	25.8 ± 2.3	51.5 ± 4.6	0.36 ± 0.05	0.21 ± 0.04
N_2 purging	N_2	1.2 ± 0.6	2.3 ± 1.1	0.07 ± 0.01	0.007 ± 0.001

[a]Experimental conditions: Under subdued light, solution were presaturated with N_2 for 2 h. Samples were then illuminated at 669 nm with O_2 bubbling (20 cm^3/min), static (no gas bubbling), or N_2 bubbling (20 cm^3/min) for 2.5 h, where $^1O_2$ was generated and detected by trapping with **1** (0.10 mM, pH = 10). The concentration of anthracene **1** was measured by monitoring the decrease of its absorption at 378 nm. [b]Initial and final rates were calculated over the first and last 30 min of the reaction, respectively. [c]The numbers shown here are averages of 3 measurements.

presaturated with N_2, little endoperoxide **2** was formed (2.3 nmol after 2.5 h); the small amount of endoperoxide observed may be due to leaks or residual oxygen in solution. These observations are in good agreement with the results of our previous work, where nitrogen purged solutions also yielded the highest rates of $^1O_2$ trapping, as evidenced either by endoperoxide **2** yield[15] or by *E. coli* deactivation.[38] The lower rate observed with $^3O_2$ purged solutions is attributed to a reduced transport of $^1O_2$ across the gas/liquid interface into the $^3O_2$ saturated solution.

Table 1 summarizes the static and sparging gas flow $^1O_2$ photoreactor experiments. The highest rate of endoperoxide **2** formation (0.96 nmol/min) occurs when $^3O_2$ is bubbled through a D_2O solution presaturated with N_2. This experimental scenario produces the highest rates as the $^1O_2$ produced has both the greatest surface area over which to contact the solution (owing to the bubbles rising through the solution) and the greatest solubility in the solution (owing to the depleted $^3O_2$ concentration resulting from N_2 presaturation). Purging the solution with oxygen before irradiation lowers the initial rate to 0.60 nmol/min. Once the solution becomes saturated in $^3O_2$, the rates decrease and become similar, regardless of the initial condition. This lower rate is similar for all oxygen-saturated systems including the final rate for solutions presaturated with either N_2 or O_2 (0.22 and 0.21 nmol/min respectively) as well as the static solution purged with $^3O_2$ (0.21 nmol/min). When $^3O_2$ is excluded, essentially no $^1O_2$ is produced (0.007 nmol/min for the last 30 min of the system with N_2 flow through a N_2 purged solution).

Effect of Pc Particle Location on Singlet Oxygen Yield. To examine the effect of particle location on $^1O_2$ trapping, a series of surfaces (A–C) was prepared where the location of the Pc particles was controlled such that the particles covered the entire surface of the posts (surface A), were restricted to the tops of the posts such that the particles were near or in contact with the solution (surface B) or were exposed only in the plastron and isolated from direct contact with solution (surface C). In this way, the relative effectiveness of $^1O_2$ generated in solution vs in the plastron could be evaluated.

The endoperoxide **2** yields for surfaces A–C were compared to each other in experiments that flowed oxygen continuously through the plastron using solutions presaturated with N_2. Table 2 shows that $^1O_2$ was trapped more effectively (factor of >2.3) when the Pc particles were located on the top of the posts in or near contact with the solution (86.3 nmol, surface B) as compared to when particles were located only in the plastron, isolated from the liquid phase (37.3 nmol, surface C). Surface A (with Pc particles coating the entire surface) resulted in the highest overall yield of trapped $^1O_2$ (97.6 nmol) as $^1O_2$ was generated both at the gas–solid interface in the plastron and at the liquid–solid interface in solution. The results clearly show that direct Pc particle contact with the solution is not required for trapping $^1O_2$; however, the yield of endoperoxide **2** is reduced by more than 60% for surface C. Unlike heterogeneous sensitizers in direct contact with the solution,[39,40] surface C may be promising for extended photolysis applications where the photodegradation of the sensitizer can be lessened because it is not in contact with solution.

Table 2. Effect of Sensitizer Location on $^1O_2$ Trapped in D_2O Solution[a]

Pc particle location	decrease of anthracene 1 (%)	endoperoxide 2 produced (nmol)
surface A (Pc located over entire surface)	48.8 ± 2.7	97.6 ± 5.3
surface B (Pc located at the tip of the posts)	43.1 ± 1.2	86.3 ± 2.7
surface C (Pc isolated from the liquid phase)	18.6 ± 0.6	37.3 ± 2.7

[a]Experiments conditions: the solution was presaturated with N_2 for 2 h prior to introducing 2.0 mL of solution into the reactor. Samples were then illuminated at 669 nm with O_2 bubbling (20 cm^3/min) for 2.5 h. Generated $^1O_2$ was detected by trapping with **1** (0.10 mM, pH = 10). The numbers shown here are averages of 3 measurements.

Mechanism of Photooxidation. The cuvette-based photoreactor is useful for elucidating the mechanism of singlet oxygen photooxidation as it enables the use of solutions presaturated with different gases as well as the independent control of the gas-phase composition, flow rate, and specific location of the sensitizer particles on the surface relative to the gas–liquid interface. Figure 9 shows our proposed mechanism. Singlet oxygen either can be generated at the gas–solid interface in the plastron, and then transported to the solution, or can be generated at the liquid-Pc interface directly in solution. In the plastron, $^3O_2$ reacts on the Pc particle surface to generate $^1O_2$. When there is no gas flow through the cuvette, $^1O_2$ must diffuse across the plastron until it enters the plastron-liquid interface where it can react with **1**. Because of the limited lifetime of $^1O_2$ only a fraction of the $^1O_2$ generated will be solvated and react with **1** before it decays to $^3O_2$. A flow of $^3O_2$ through the plastron increases the yield of $^1O_2$ trapped in solution by two mechanisms. First oxygen gas flow increases the concentration of $^3O_2$ on the catalyst surface, thereby increasing the overall quantity of $^1O_2$ formed. Higher concentrations of $^3O_2$ are known to increase the yields of $^1O_2$ in the presence of a photosensitizer.[41] Second, the $^1O_2$ generated in the plastron will be transported more efficiently into contact with solution due to the gas flow which creates bubbles that rise through the solution, thereby increasing the

dx.doi.org/10.1021/jp503149x | J. Phys. Chem. A 2014, 118, 10364–10371

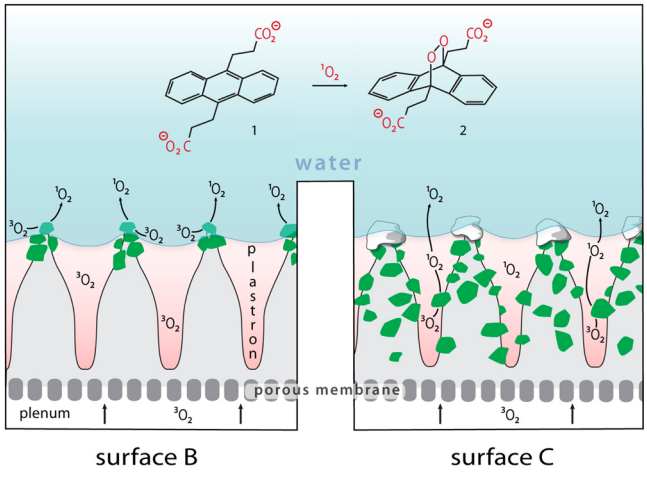

Figure 9. Mechanism of singlet oxygen generation via O_2 flowing through the plastron of a superhydrophobic sensitizer surface.

liquid–gas interfacial area. This increases the opportunity for $^1O_2$ to become solvated and react with **1** before it decays. Indeed, we observe the highest rates of endoperoxide **2** formation in the presence of flowing $^3O_2$. Results from surface C demonstrate that this mechanism, alone, can result in singlet oxygen trapping.

When Pc particles are in contact with the solution (surfaces A and B), a second mechanism for generating $^1O_2$ is operational. Oxygen ($^3O_2$) dissolved in solution will react at the particle-solution interface to generate $^1O_2$ directly in solution where it can diffuse and be trapped by reacting with **1**. Increasing the $^3O_2$ concentration dissolved in solution would again increase the yield of $^1O_2$ trapped. This was observed for static solutions presatured with $^3O_2$.

For flowing $^3O_2$ experiments, however, presaturation of the solution with N_2 proved to be more effective than presaturation with $^3O_2$. Initial rates of endoperoxide **2** formation were higher for N_2 vs $^3O_2$ presaturation (0.96 vs 0.60 nmol/min). In this condition, the solubility and diffusion of $^1O_2$ into solution will be more rapid when the concentration of dissolved $^3O_2$ is lower (Fick's Law).[42] As the concentration of dissolved oxygen in solution increases, singlet oxygen solubility from the bubble into solution will decrease, slowing the overall trapping rate; reactions of singlet oxygen present in bubbles would ultimately be limited to the gas–liquid interface. This was reflected by the lower final rates of endoperoxide formation (~0.21 nmol/min regardless of presaturation level). We observed a similar effect of solution presaturation (i.e., higher rates with N_2 vs $^3O_2$ solution presaturation) using a very different type of singlet oxygen generator.[15]

The generation of singlet oxygen in solution at the Pc particle–solution interface accounts for the majority of the trapped $^1O_2$. This mechanism prevails even when solutions are presaturated with N_2, because $^3O_2$ can rapidly diffuse from the plastron to this interface during $^3O_2$ purging. Only when the dissolved $^3O_2$ content is reduced will the rate of $^1O_2$ generation in solution be reduced. This was observed for N_2 presaturated solutions in static air, especially at the end of the 150 min experiment when $^3O_2$ would have been depleted from the plastron.

By control of the location of particles on the surface, illustrated by the synthesis of surfaces A–C, the mechanistic significance of these two nonequivalent $^1O_2$-generating regions is revealed. The observations of our experiments are consistent with the short lifetime of $^1O_2$ and the transport mechanisms involved. When $^1O_2$ is generated at the top of the PDMS posts, the distance over which the singlet oxygen must diffuse to encounter **1** is relatively short as $^1O_2$ either is generated in solution or can easily diffuse to the liquid–gas interface. When generated in the plastron, however, $^1O_2$ is first transported via a bubble into the liquid layer where it must be solvated and diffuse to and encounter **1** before decaying back to the ground state. Flowing gas enhances the transport of $^1O_2$ into solution, and thus the yield of **2**, as compared to an environment in which, for example, an individual droplet of solution[16] rests on a superhydrophobic surface embedded with Pc particles in static air.

CONCLUSION

Physical-organic studies were used to investigate superhydrophobic sensitizer surfaces coupled into a photoreactor device so that the layer of gas trapped between the surface and the liquid could be enriched with oxygen. This superhydrophobic surface device is especially well suited for such studies as it enables control of the sensitizer particle location relative to the solution as well as provides facile access to the plastron. Because of the hierarchical texture on the printed surface, a stable Cassie state was maintained throughout the experiment; the Pc particles partially embedded into the PDMS posts required no special surface treatment to maintain superhydrophobicity. Fabrication of these surfaces is inexpensive, scalable and easily adaptable to a wide range of catalyst particles.

The endoperoxide **2** is the sole product from the reaction of singlet oxygen with anthracene **1**. When oxygen flows continuously through the plastron, the efficiency of singlet oxygen trapping increases significantly as compared to the static plastron environment. By contrast, flowing N_2 through the plastron essentially precluded endoperoxide formation. By studying surfaces where the catalyst particles are proximate to, or isolated from, the aqueous solution (surfaces A–C), we determined the relative efficiency of $^1O_2$ trapping. Singlet oxygen generated directly in solution is trapped more efficiently resulting in >60% higher yields. However, we clearly demonstrated that $^1O_2$ can be trapped in solution with reasonable yields (~37 nmol) even when the sensitizer Pc particles are physically separated from the solution.

Can this cuvette technology driven by physical-organic principles enlarge the tool set for $^1O_2$ in synthesis[43] or to deliver $^1O_2$? We have taken an approach where surface printing and sensitizer configuration technology may be advantageous in applications such as water purification and medical devices where gas-phase generation of singlet oxygen is desired, but contamination of the fluid by the photocatalyst, or conversely, contamination of the photocatalyst by the solution, must be avoided. Supporting fluid in the Cassie state may also be ideal for applications where the surfaces are intended for long-term use to restrict contact points for growth of bacteria and the formation of biofilms that may cause infections.[44] In addition, $^1O_2$ generated at the gas–solid interface will effectively kill bacteria[38] resulting in self-cleaning surfaces that can efficiently purify water.

dx.doi.org/10.1021/jp503149x | J. Phys. Chem. A 2014, 118, 10364–10371

■ ASSOCIATED CONTENT

Supporting Information

Video of the bubble cycle with $^1O_2$ bubble forming and releasing from the plastron-liquid interface. This material is available free of charge via the Internet at http://pubs.acs.org.

■ AUTHOR INFORMATION

Notes

The authors declare no competing financial interest.

■ ACKNOWLEDGMENTS

Y.Z., Y.L., Q.X., M.B., and A.M.L. acknowledge support from the NYS Empire State Development's Division of Science, Technology & Innovation (NYSTAR) and the CUNY Center for Advanced Technology. M.B. also acknowledges support from the National Science Foundation (STEP 0653056). D.B. and A.G. acknowledge support from the National Institute of General Medical Sciences (NIH SC1GM093830). We thank Michael Bucaro for assistance with the SEM imaging and Leda Lee for the graphic arts work.

■ REFERENCES

(1) Clennan, E. L.; Pace, A. Advances in Singlet Oxygen Chemistry. *Tetrahedron* **2005**, *61*, 6665−6691.
(2) Kruft, B. I.; Greer, A. Photosensitized Reactions In Vitro and In Vivo. *Photochem. Photobiol.* **2011**, *87*, 1204−1213.
(3) Jirasek, V.; Censky, M.; Spalek, O.; Kodymová, J. High-Pressure Generator of Singlet Oxygen. *Chem. Eng. Technol.* **2013**, *36*, 1755−1763.
(4) Wootton, R. C. R.; Fortt, R.; deMello, A. J. A Microfabricated Nanoreactor for Safe, Continuous Generation and Use of Singlet Oxygen. *Org. Process Res. Dev.* **2002**, *6*, 187−189.
(5) Coyle, E. E.; Oelgemöller, M. Micro-Photochemistry: Photochemistry in Microstructured Reactors. The New Photochemistry of the Future? *Photochem. Photobiol. Sci.* **2008**, *7*, 1313−1322.
(6) Yavorskyy, A.; Shvydkiv, O.; Nolan, K.; Hoffmann, N.; Oelgemöller, M. Photosensitized Addition of Isopropanol to Furanones in a Continuous-Flow Dual Capillary Microreactor. *Tetrahedron Lett.* **2011**, *52*, 278−280.
(7) Lévesque, F.; Seeberger, P. H. Highly Efficient Continuous Flow Reactions Using Singlet Oxygen as a "Green" Reagent. *Org. Lett.* **2011**, *13*, 5008−5011.
(8) Lumley, E. K.; Dyer, C. E.; Pamme, N.; Boyle, R. W. Comparison of Photo-Oxidation Reactions in Batch and a New Photosensitizer-Immobilized Microfluidic Device. *Org. Lett.* **2012**, *14*, 5724−5727.
(9) Elvira, K. S.; Wootton, R. C. R.; Reis, N. M.; Mackley, M. R.; deMello, A. J. Through-Wall Mass Transport as a Modality for Safe Generation of Singlet Oxygen in Continuous Flows. *ACS Sustainable Chem. Eng.* **2013**, *1*, 209−213.
(10) Yoon, H. K.; Lou, X.; Chen, Y.-C.; Lee, Y.-E. Y.; Yoon, E.; Kopelman, R. Nanophotosensitizers Engineered to Generate a Tunable Mix of Reactive Oxygen Species, for Optimizing Photodynamic Therapy, Using a Microfluidic Device. *Chem. Mater.* **2014**, *26*, 1592−1600.
(11) Hou, L.; Zhang, X.; Pijper, T. C.; Browne, W. R.; Feringa, B. L. Reversible Photochemical Control of Singlet Oxygen Generation Using Diarylethene Photochromic Switches. *J. Am. Chem. Soc.* **2014**, *136*, 910−913.
(12) Zhou, L.; Wei, S.; Ge, X.; Zhou, J.; Yu, B.; Shen, J. External Heavy-Atomic Construction of Photosensitizer Nanoparticles for Enhanced in Vitro Photodynamic Therapy of Cancer. *J. Phys. Chem. B* **2012**, *116*, 12744−12749.
(13) Henke, P.; Lang, K.; Kubát, P.; Sýkora, J.; Šlouf, M.; Mosinger, J. Polystyrene Nanofiber Materials Modified with an Externally Bound Porphyrin Photosensitizer. *ACS Appl. Mater. Interfaces* **2013**, *5*, 3776−3783.
(14) Parthasarathy, A.; Goswami, S.; Corbitt, T. S.; Ji, E.; Dascier, D.; Whitten, D. G.; Schanze, K. S. Photophysics and Light-Activated Biocidal Activity of Visible-Light-Absorbing Conjugated Oligomers. *ACS Appl. Mater. Interfaces* **2013**, *5*, 4516−4520.
(15) Bartusik, D.; Aebisher, D.; Ghafari, B.; Lyons, A. M.; Greer, A. Generating Singlet Oxygen Bubbles: A New Mechanism for Gas-Liquid Oxidations in Water. *Langmuir* **2012**, *28*, 3053−3060.
(16) Aebisher, D.; Bartusik, D.; Liu, Y.; Zhao, Y.; Barahman, M.; Xu, Q.; Lyons, A. M.; Greer, A. Superhydrophobic Photosensitizers. Mechanistic Studies of $^1O_2$ Generation in the Plastron and Solid/Liquid Droplet Interface. *J. Am. Chem. Soc.* **2013**, *135*, 18990−18998.
(17) Cassie, A. B. D.; Baxter, S. Wettability of Porous Surfaces. *Trans. Faraday Soc.* **1944**, *40*, 546−551.
(18) Ranby, B.; Rabek, J. F. *Singlet Oxygen: Reactions with Organic Compounds and Polymers*; Wiley-Interscience: New York, 1978.
(19) Bourdelande, J. L.; Karzazi, M.; Dicelio, L. E.; Litter, M. I.; Tura, G. M.; Román, E. S.; Vinent, V. Phthalocyanines Bound to Insoluble Polystyrene. Synthesis and Properties as Engergy-Transfer Photosensitizers. *J. Photochem. Photobiol., A* **1997**, *108*, 273−282.
(20) Kim, J.; Rodriguez, M. E.; Oleinick, N. L.; Anderson, V. E. Photo-Oxidation of Cardiolipin and Cytochrome *c* with Bilayer-Embedded Pc 4. *Free Radical Biol. Med.* **2010**, *49*, 718−725.
(21) Barahman, M.; Lyons, A. M. Ratchetlike Slip Angle Anisotropy on Printed Superhydrophobic Surfaces. *Langmuir* **2011**, *27*, 9902−9909.
(22) Xu, Q.; Liu, Y.; Lin, F.-J.; Mondal, B.; Lyons, A. M. Superhydrophobic TiO_2-Polymer Nanocomposite Surface with UV-Induced Reversible Wettability and Self-Cleaning Properties. *ACS Appl. Mater. Interfaces* **2013**, *5*, 8915−8924.
(23) Koch, K.; Bhushan, B.; Jung, Y. C.; Barthlott, W. Fabrication of Artificial Lotus Leaves and Significance of Hierarchical Structure for Superhydrophobicity and Low adhesion. *Soft Matter* **2009**, *5*, 1386−1393.
(24) Wenzel, R. N. Resistance of Solid surfaces to Wetting by Water. *Ind. Eng. Chem.* **1936**, *28*, 988−994.
(25) Lafuma, A.; Quéré, D. Superhydrophobic States. *Nat. Mater.* **2003**, 457−460.
(26) Sun, W.; Zhou, S.; Chen, P.; Peng, L. Reversible Switching on Superhydrophobic TiO_2 Nano-Strawberry Films Fabricated at Low Temperature. *Chem. Commun.* **2008**, *2*, 603−605.
(27) Lindig, B. A.; Rodgers, M. A. J.; Schaap, A. P. Determination of the Lifetime of Singlet Oxygen in D_2O Using 9,10-Anthracenedipropionic Acid, a Water-Soluble Probe. *J. Am. Chem. Soc.* **1980**, *102*, 5590−5593.
(28) Lindig, B. A.; Rodgers, M. A. J. Rate Parameters for the Quenching of Singlet Oxygen by Water-Soluble and Lipid-Soluble Substrates in Aqueous and Micellar Systems. *Photochem. Photobiol.* **1981**, *33*, 627−634.
(29) Brauer, H.-D.; Schmidt, R. Comment on "New Assignment of the Electronically Excited States of Anthracene-9,10-Endoperoxide and Its Derivatives: A Critical Experimental and Theoretical Study". *J. Phys. Chem. A* **2000**, *104*, 164−165.
(30) Fuchter, M. J.; Hoffman, B. M.; Barrett, A. G. M. Ring-Opening Metathesis Polymer Sphere-Supported *seco*-Porphyrazines: Efficient and Recyclable Photooxygenation Catalysts. *J. Org. Chem.* **2006**, *71*, 724−729.
(31) Fudickar, W.; Linker, T. Novel Anthracene Materials for Application in Lithography and Reversible Photoswitching by Light and Air. *Langmuir* **2010**, *26*, 4421−4428.
(32) Oliveira, M. S.; Severino, D.; Prado, F. M.; Angeli, J. P. F.; Motta, F. D.; Baptista, M. S.; Medeiros, M. H. G.; Di Mascio, P. Singlet Molecular Oxygen Trapping by the Fluorescent Probe Diethyl-3,3′-(9,10-anthracenediyl)bisacrylate Synthesized by the Heck Reaction. *Photochem. Photobiol. Sci.* **2011**, *10*, 1546−1555.
(33) Balta, D. K.; Temel, G.; Goksu, G.; Ocal, N.; Arsu, N. Thioxanthone-Diphenyl Anthracene: Visible Light Photoinitiator. *Macromolecules* **2012**, *45*, 119−125.
(34) Anula, H. M.; Berlin, J. C.; Wu, H.; Li, Y.-S.; Peng, X.; Kenney, M. E.; Rodgers, M. A. J. Sythesis and Photophysical Properties of

Silicon Phthalocyanines with Axial Siloxy Ligands Bearing Alkylamine Termini. *J. Phys. Chem. A* **2006**, *110*, 5215−5223.
(35) Ravanat, J.-L.; Berger, M.; Benard, F.; Langlois, R.; Ouellet, R.; Van Lier, J. E.; Cadet, J. Phthalocyanine and Naphthalocyanine Photosensitized Oxidation of 2′-Deoxyguanosine. *Photochem. Photobiol.* **1992**, *55*, 809−814.
(36) Tuncel, S.; Dumoulin, F.; Gailer, J.; Sooriyaarachchi, M.; Atilla, D.; Durmus, M.; Bouchu, D.; Savoie, H.; Boyle, R. W.; Ahsen, V. A Set of Highly Water-Soluble Tetraethyleneglycol-Substituted Zn(II) Phthalocyanines: Synthesis, Photochemical and Photophysical Properties, Interaction with Plasma Proteins and *In Vitro* Phototoxicity. *Dalton Trans.* **2011**, *40*, 4067−4079.
(37) Jensen, R. L.; Arnbjerg, J.; Ogilby, P. R. Temperature Effects on the Solvent-Dependent Deactivation of Singlet Oxygen. *J. Am. Chem. Soc.* **2010**, *132*, 8098−8105.
(38) Bartusik, D.; Aebisher, D.; Lyons, A. M.; Greer, A. Bacterial Inactivation by a Singlet Oxygen Bubbler: Identifying Factors Controlling the Toxicity of $^1O_2$ Bubbles. *Environ. Sci. Technol.* **2012**, *46*, 12098−12104.
(39) Enko, B.; Borisov, S. M.; Regensburger, J.; Bäumler, W.; Gescheidt, G.; Klimant, I. Singlet Oxygen-Induced Photodegradation of the Polymers and Dyes in Optical Sensing Materials and the Effect of Stabilizers on These Processes. *J. Phys. Chem. A* **2013**, *117*, 8873−8882.
(40) Giaimuccio, J.; Zamadar, M.; Aebisher, D.; Meyer, G. J.; Greer, A. Singlet Oxygen Chemistry in Water. 2. Photoexcited Sensitizer Quenching by O_2 at the Water-Porous Glass Interface. *J. Phys. Chem. B* **2008**, *112*, 15646−15650.
(41) Hatz, S.; Poulsen, L.; Ogilby, P. R. Time-resolved Singlet Oxygen Phosphorescence Measurements from Photosensitized Experiments in Single Cells: Effects of Oxygen Diffusion and Oxygen Concentration. *Photochem. Photobiol.* **2008**, *84*, 184−1290.
(42) Tromans, D. Modeling Oxygen Solubility in Water and Electrolyte Solutions. *Ind. Eng. Chem. Res.* **2000**, *39*, 805−812.
(43) Protti, S.; Dondi, D.; Fagnoni, M.; Albini, A. Photochemistry in Synthesis: Where, When, and Why. *Pure Appl. Chem.* **2007**, *79*, 1929−1938.
(44) Li, J.; Liu, X.; Qiao, Y.; Zhu, H.; Li, J.; Cui, T.; Ding, C. Enhanced Bioactivity and Bacteriostasis Effect of TiO_2 Nanofilms with Favorable Biomimetic Architectures on Titanium Surface. *RSC Adv.* **2013**, *3*, 11214−11225.